

Diffusion-based Virtual Fixtures

Cem Bilaloglu, Tobias Löw, and Sylvain Calinon

Abstract—Virtual fixtures assist human operators in teleoperation settings by constraining their actions. This extended abstract introduces a novel virtual fixture formulation *on surfaces* for tactile robotics tasks. Unlike existing methods, our approach constrains the behavior based on the position on the surface and generalizes it over the surface by considering the distance (metric) on the surface. Our method works directly on possibly noisy and partial point clouds collected via a camera. Given a set of regions on the surface together with their desired behaviors, our method diffuses the behaviors across the entire surface by taking into account the surface geometry. We demonstrate our method’s ability in two simulated experiments (i) to regulate contact force magnitude or tangential speed based on surface position and (ii) to guide the robot to targets while avoiding restricted regions defined on the surface. All source codes, experimental data, and videos are available as open access at <https://sites.google.com/view/diffusion-virtual-fixtures>.

Index Terms—Virtual Fixtures, Tactile Robotics

I. INTRODUCTION

For a long time, robotics considered objects in the environment primarily as obstacles and the goal was to avoid contact due to modeling and sensing difficulties. However, the trend has shifted towards embracing contact due to increasing interest in manipulation, tactile robotics, and surface inspection tasks. Consequently, robots physically interact with their surrounding environment that can be characterized by curved surfaces, which can also be soft and fragile (e.g., surgical robotics). However, safety in these tasks remains a major concern during deployment in real-world as they involve forceful interactions. Considering that a significant percentage of recent approaches propose learning-based controllers, and that the majority of shared control and teleoperation tasks depend on the operator’s expertise or skills, safety takes a more central role in assistive systems. Therefore, in tactile tasks, there is a need for modules that can be combined with other controllers to enforce high priority constraints.

Virtual fixtures, introduced by Rosenberg [1] for teleoperation, are formulations that assist the operator by constraining their actions. Existing methods [2]–[6], although operating on surfaces, consider the problem in the robot workspace with the standard Euclidean metric. Accordingly, they do not capture the tangent space and the distance (metric) on the surface. In contrast, various tactile tasks have constraints based on the position on the surface instead of a single guidance path and they change based on the distance on the surface. For instance, to regulate the contact force magnitude or the speed based on the position on the surface, one can annotate the desired values at particular points, as shown in Figure 1-a. Then, these values can be diffused by considering the surface metric across the entire surface as in Figure 1-b. Alternatively, by

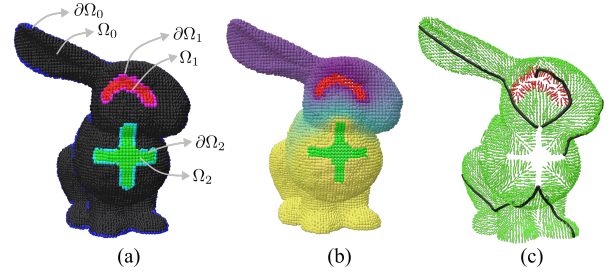


Fig. 1: Input and example use-cases of our method. Left, the input to our method – a partial point cloud with segmented regions Ω_1 , Ω_2 and the free region Ω_0 with their estimated boundaries $\partial\Omega_1$, $\partial\Omega_2$ and $\partial\Omega_0$. Center, the first experiment showing the virtual fixture constraining the contact force magnitude based on diffusing the contact forces designated on Ω_1 and Ω_2 . Right, the second experiment showing the flow field guiding the agents towards target Ω_2 by avoiding restricted regions Ω_1 where the black paths show trajectories with different initial positions.

specifying only the target and obstacle regions, a smooth flow field on the tangent space can guide agents to the closest target while avoiding the restricted zones and maintaining contact with the surface, as depicted in Figure 1-c. For addressing these challenges, we propose a surface virtual fixture method expecting surfaces as possibly noisy and partial point clouds collected in runtime using an off-the-shelf camera attached to the robot. Next, we segment the point cloud into a set of regions with their specified behavior. This segmentation can come from learning-based methods using vision [7] or geometry [8]. Alternatively, one can use virtual or real-world expert annotations [5], [6], possibly in combination with feature extractors [4]. Then, we diffuse the specified behavior across the whole surface to combine them consistently by considering the surface metric.

II. METHOD

We assume the surfaces that we interact with are two-dimensional Riemannian manifolds \mathcal{M} that we can measure using an RGB-D camera. Accordingly, we can represent them as *point clouds*

$$\Omega := \left\{ (\mathbf{p}_i, \mathbf{c}_i) \mid \begin{array}{l} \mathbf{p}_i \in \mathcal{M}, \mathbf{c}_i \in \{0, \dots, 255\}^3 \\ \text{for } i = 1, \dots, n_{\mathcal{P}} \end{array} \right\} \quad (1)$$

where \mathbf{p}_i are the point positions and \mathbf{c}_i are the RGB color intensities. As explained in the introduction we can find a mapping from \mathbf{p}_i and \mathbf{c}_i to a set of specified behaviors $\Phi := \{\phi_1, \dots, \phi_i, \dots, \phi_N\}$ on these points. We assume the

union of points with the same specified behavior ϕ_i composes a region Ω_i on the manifold. We consider all the points that do not have a specified behavior as the free region and denote it with Ω_0 . Therefore we segment our manifold \mathcal{M} into $N+1$ disjoint regions. Next, we estimate the boundaries of these regions using the procedure implemented by the *PCL* library and we designate the boundary of the i -th region using $\partial\Omega_i$. We provide an example with $N=2$ in Figure 1-a.

Our method aims to generalize the correct behavior to free region Ω_0 given a sparse set of behaviors in Ω_i considering the metric of the surface. For that purpose, we solve the diffusion equation

$$\dot{u}(\mathbf{x}, t) = \mathbf{L}u(\mathbf{x}, t) \quad \text{on } \Omega, \quad (2)$$

where $u(\mathbf{x}, t) : \Omega \rightarrow \mathbb{R}$ is the scalar field at time t resulting from diffusing the initial field $u(\mathbf{x}, 0)$ and \mathbf{L} denotes the Laplace-Beltrami operator generalizing the Laplacian Δ to the Riemannian manifolds. Note that a partial differential equation only specifies the behavior on the interior of the domain, and for the desired unique solution one specifies the behavior at the boundary

$$u(\mathbf{x}) = g(\mathbf{x}) \quad \text{on } \partial\Omega_D, \quad \frac{\partial u(\mathbf{x})}{\partial n_x} = h(\mathbf{x}) \quad \text{on } \partial\Omega_N, \quad (3)$$

where $\partial\Omega_D$ and $\partial\Omega_N$ correspond to the Dirichlet and Neumann boundaries, respectively. We assume the designated behaviors fix the boundary conditions on the neighboring boundaries of the free region (see cyan and magenta regions in Figure 1-a). However, there might be also additional boundaries without specified behavior (e.g., blue regions in Figure 1-a). In that case, we assume the boundary to be zero Neumann $h(\mathbf{x}) = 0$, meaning no information diffuses through the boundary.

Note that the solution of the diffusion equation (2) depends on the diffusion time t_D . After a sufficient time $t_D \gg 0$ the diffusion reaches a steady-state where the time derivative vanishes $\dot{u}(\mathbf{x}, t) = 0$. If we plug this condition into the diffusion equation (2), we recover the steady-state diffusion equation (i.e., Laplace's equation)

$$\mathbf{L}u(\mathbf{x}) = 0 \quad \text{on } \Omega. \quad (4)$$

Laplace's equation (4) minimizes the Dirichlet energy, thus providing the smoothest possible interpolation of the Dirichlet boundary conditions to the interior of the domain. Similarly, the transient diffusion (2) provides a locally smooth interpolation, where the radius of the local zone is determined by the diffusion time t_D . In the limiting case where $t_D \rightarrow 0$ it is shown that one can recover geodesics [9] and interpolate the boundary data based on the geodesic distance. We use the diffusion time as the hyperparameter of our method to select the desired smoothness of the results.

III. EXPERIMENTS

For the experiments, we used the partial and noisy point cloud of the Stanford bunny, and we assumed an expert marked the regions Ω_1 and Ω_2 as shown in Figure 1-a.

As the first experiment, we considered a task where the robot needs to apply contact forces F_1 and F_2 in Ω_1 and Ω_2 respectively. Then, we solved Laplace's equation using F_1 and F_2 as Dirichlet boundary conditions on the $\partial\Omega_{1D}$ and $\partial\Omega_{2D}$ to find the contact forces interpolating the values to Ω_0 as shown in Figure 1 b.

For the second task, we considered target-reaching and obstacle-avoidance on the surface. We specified the desired behavior as follows:

- Obstacles Ω_1 push the agents on their interior and do not affect the agents on their exterior.
- Targets Ω_2 do not affect the agents in their interior and pull the agents on their exterior.
- The free region Ω_0 guides the agents toward targets Ω_2 without passing through the obstacles Ω_1

and satisfy these behaviors using two independent virtual fixtures. First, for obstacle avoidance, we solved the diffusion equation (2) in the region Ω_1 where we set the Dirichlet boundary as $\partial\Omega_{1D} = 1$ and started from the initial condition $u(\mathbf{x}, 0) = \mathbf{0}$ in Ω_1 . This leads to the gradients in the region ∇_x , $\mathbf{x} \in \Omega_1$ point towards the exterior $\nabla_x = \mathbf{n}_x$ where \mathbf{n}_x are the unit vectors pointing outward from the region.

Secondly, for target reaching, we solved the diffusion equation (2) in the combined region $\Omega_0 \cup \partial\Omega_2$, where we set the Dirichlet boundary $\partial\Omega_{2D} = 1$ and the Neumann boundary $\partial\Omega_{0N} = \mathbf{0}$, starting from the initial condition $u(\mathbf{x}, 0) = \mathbf{0}$ in Ω_0 . Accordingly, the gradients at the boundary of the target ∇_x , $\mathbf{x} \in \partial\Omega_2$ point towards the target interior $\nabla_x = -\mathbf{n}_x$. Note that the zero Neumann boundary condition ensures that none of the gradients at the boundary of the free region ∇_x , $\mathbf{x} \in \partial\Omega_0$ would point towards the obstacle region or out of the surface. As recommended by [9], we set the time parameter $t_D = h^2$, where h is the mean distance between the neighboring points in the point cloud.

IV. CONCLUSION & FUTURE WORK

We presented a novel virtual fixture method on surfaces based on mature tools from the partial differential equations and computer graphics literature for addressing tactile robotics tasks [9], [10]. We demonstrated our approach based on diffusing scalar valued functions on surfaces is promising for generalizing the desired behavior defined in some regions to the whole surface, by considering the metric of the surface.

A natural extension of our work is to consider diffusion of vector-valued data [11], [12] such that we can use it for diffusing velocities on the tangent space or to diffuse orientations by using the Lie algebra of the unit quaternion group. Alternatively, we can consider bivectors to diffuse the specified dynamical behaviors [13], [14] at particular regions to the whole domain. Another promising direction is to extend our approach from surfaces to other domains such as the workspace \mathbb{R}^3 or the joint space of the robot endowed with a non-Euclidean metric, using Monte Carlo methods for solving the diffusion [15]–[17].

REFERENCES

- [1] L. Rosenberg, “Virtual fixtures: Perceptual tools for telerobotic manipulation,” in *Proceedings of IEEE Virtual Reality Annual International Symposium*, Seattle, WA, USA: IEEE, 1993, pp. 76–82. DOI: 10.1109/VRAIS.1993.380795.
- [2] M. Selvaggio, G. A. Fontanelli, F. Ficuciello, L. Villani, and B. Siciliano, “Passive Virtual Fixtures Adaptation in Minimally Invasive Robotic Surgery,” *IEEE Robotics and Automation Letters*, vol. 3, no. 4, pp. 3129–3136, Oct. 2018. DOI: 10.1109/LRA.2018.2849876.
- [3] M. Mühlbauer, T. Hulin, B. Weber, *et al.*, “A Probabilistic Approach to Multi-Modal Adaptive Virtual Fixtures,” *IEEE Robotics and Automation Letters*, vol. 9, no. 6, pp. 5298–5305, Jun. 2024. DOI: 10.1109/LRA.2024.3384759.
- [4] V. Pruks and J.-H. Ryu, “Method for generating real-time interactive virtual fixture for shared teleoperation in unknown environments,” *The International Journal of Robotics Research*, vol. 41, no. 9-10, pp. 925–951, Aug. 2022. DOI: 10.1177/02783649221102980.
- [5] C. P. Quintero, S. Li, M. K. Pan, W. P. Chan, H. Machiel Van Der Loos, and E. Croft, “Robot Programming Through Augmented Trajectories in Augmented Reality,” in *2018 IEEE/RSJ International Conference on Intelligent Robots and Systems (IROS)*, Madrid: IEEE, Oct. 2018, pp. 1838–1844. DOI: 10.1109/IROS.2018.8593700.
- [6] C. P. Quintero, M. Dehghan, O. Ramirez, M. H. Ang, and M. Jagersand, “Flexible virtual fixture interface for path specification in tele-manipulation,” in *2017 IEEE International Conference on Robotics and Automation (ICRA)*, Singapore: IEEE, May 2017, pp. 5363–5368. DOI: 10.1109/ICRA.2017.7989631.
- [7] M. Caron, H. Touvron, I. Misra, *et al.* “Emerging Properties in Self-Supervised Vision Transformers.” (May 24, 2021), [Online]. Available: <http://arxiv.org/abs/2104.14294> (visited on 07/06/2024), pre-published.
- [8] N. Sharp, S. Attaiki, K. Crane, and M. Ovsjanikov, “DiffusionNet: Discretization Agnostic Learning on Surfaces,” *ACM Transactions on Graphics*, vol. 41, no. 3, 27:1–27:16, Mar. 7, 2022. DOI: 10.1145/3507905.
- [9] K. Crane, C. Weischedel, and M. Wardetzky, “Geodesics in heat: A new approach to computing distance based on heat flow,” *ACM Transactions on Graphics*, vol. 32, no. 5, 152:1–152:11, Oct. 8, 2013. DOI: 10.1145/2516971.2516977.
- [10] M. Belkin, J. Sun, and Y. Wang, “Constructing Laplace Operator from Point Clouds in \mathbb{R}^d ,” in *Proceedings of the Twentieth Annual ACM-SIAM Symposium on Discrete Algorithms*, Society for Industrial and Applied Mathematics, Jan. 4, 2009, pp. 1031–1040. DOI: 10.1137/1.9781611973068.112.
- [11] N. Sharp, Y. Soliman, and K. Crane, “The Vector Heat Method,” *ACM Transactions on Graphics*, vol. 38, no. 3, pp. 1–19, Jun. 30, 2019. DOI: 10.1145/3243651.
- [12] D. Robert-Nicoud, A. Krause, and V. Borovitskiy. “Intrinsic Gaussian Vector Fields on Manifolds.” (Mar. 31, 2024), [Online]. Available: <http://arxiv.org/abs/2310.18824> (visited on 05/06/2024), pre-published.
- [13] B. Fichera and A. Billard, “Hybrid Quadratic Programming – Pullback Bundle Dynamical Systems Control,” in vol. 27, 2023, pp. 387–394. DOI: 10.1007/978-3-031-25555-7_26.
- [14] B. Fichera and A. Billard. “Learning Dynamical Systems Encoding Non-Linearity within Space Curvature.” (Mar. 18, 2024), [Online]. Available: <http://arxiv.org/abs/2403.11948> (visited on 07/06/2024), pre-published.
- [15] R. Sawhney, D. Seyb, W. Jarosz, and K. Crane, “Grid-free Monte Carlo for PDEs with spatially varying coefficients,” *ACM Transactions on Graphics*, vol. 41, no. 4, pp. 1–17, Jul. 2022. DOI: 10.1145/3528223.3530134.
- [16] K. K. Sabelfeld, “Random walk on rectangles and parallelepipeds algorithm for solving transient anisotropic drift-diffusion-reaction problems,” *Monte Carlo Methods and Applications*, vol. 25, no. 2, pp. 131–146, Jun. 1, 2019. DOI: 10.1515/mcma-2019-2039.
- [17] R. I. C. Muchacho and F. T. Pokorny. “Walk on Spheres for PDE-based Path Planning.” (Jun. 3, 2024), [Online]. Available: <http://arxiv.org/abs/2406.01713> (visited on 06/20/2024), pre-published.